Journal of Cultural Heritage 67 (2024) 541–552

Contents lists available at ScienceDirect

Journal of Cultural Heritage

journal homepage: www.elsevier.com/locate/culher

Original article

Systematization proposal for the analysis of columns from point clouds

Agustí Costa-Jover[a,b,*], Amparo Núñez Andrés[a], Felipe Buill Pozuelo[a], David Moreno Garcia[b], Sergio Coll-Pla[b]

[a] Escola Tècnica Superior d'Arquitectura (ETSA), Universitat Rovira i Virgili, 43204, Tarragona, Spain
[b] Department of Civil and Environmental Engineering, Division of Geotechnical Engineering and Geosciences, Universitat Politècnica de Catalunya-BarcelonaTech, 08028, Barcelona, Spain

ARTICLE INFO

Article history:
Received 29 August 2023
Accepted 24 April 2024
Available online 14 May 2024

Keywords:
Point cloud
Formal anomalies
Column
Massive data capture techniques

ABSTRACT

The research is framed in the significant development of massive data capture techniques in the 21st century, with point clouds becoming essential in various fields. In the context of architectural heritage, this topographical information is particularly useful in identifying and analysing formal anomalies, among many other applications. The study focuses on systematizing the analysis of columns, vital structural elements with diverse formal definitions, especially in historical buildings. The research proposes a simple workflow based mainly on open-source software for the systematic formal study columns. The investigation explores two types of formal anomalies, namely buckling and bulging, testing different methodological approaches. The results offer insights into the advantages and disadvantages of the proposed methods, enabling detailed parameterization of the analysed anomalies. That information is crucial from the point of view of diagnosis and conservation.

1. Introduction

The techniques for the massive capture of spatial information have undergone significant development throughout the twenty-first century. Notably, digital photogrammetry and terrestrial laser scanning sensors (TLS) have emerged as prominent methods. Currently, these techniques allow for the acquisition of high-resolution and high-precision point clouds in a relatively short period of time and non-invasively.

These data can be exploited from various disciplines. Focusing on the field of architectural heritage, these techniques often become the sole feasible approach to achieve a comprehensive and precise survey within a relatively short timeframe. Complex and irregular shapes are common in this type of constructions, which are frequently characterized by its large scale, making certain elements inaccessible. Numerous investigations have tested the technique's reliability to survey a building's geometry [1-4].

Obtaining topographic information regarding the present condition of construction elements is a key feature with multiple applications, ranging from the definition of preventive or intervention-based conservation strategies, if necessary, to historical and stylistic studies and classification, among others. In recent years, technical advancements have significantly expanded the array of possibilities for analysing these construction elements. A full overview about laser scanner and the software to work with can be found in [5].

The article proposes the systematization of the analysis process of formal anomalies in ancient buildings, with a workflow that is as simple as possible. Many studies have developed effective procedures using point cloud data to address that issue in ancient structures. [6] and [7] analyse the deformations of churches from a TLS survey, using graphic primitives and two-dimensional sections. [8] presents several case studies for the analysis of deformations from a point cloud by TLS, such as the leaning of walls from a vertical comparison plane or the leaning of a tower from finding the barycentre axis. [9] performs the deviation analysis, based on a survey with TLS of a minaret by means of sections every certain height, and from the centre of each section establishes the central axis. It is also analysed from the cone that best approximates the element, but the method used is not delved into. [10] develops a method for the analysis of displacements in a tower building

* Corresponding author.
E-mail address: agusti.costa@urv.cat (A. Costa-Jover).

https://doi.org/10.1016/j.culher.2024.04.017

from a 3D model obtained by photogrammetry with UAV imagery. It is also remarkable the recent work in Notre Dame of Paris [11], where simple procedures were needed to provide information in short time, but with sufficient precision to analyse the construction after the fire from different datasets. Moreover [12], integrates BIM (Building Information Model) modelling processes with deformation analysis via open source software such as CloudCompare from digital twins, which allows for a global analysis of formal anomalies between the reference model and the point cloud. It is an operation that combines different programs, in which specialized knowledge is necessary. Many of these examples propose similar strategies, but in each case the analysis is resolved with different methods and programs, adapted to the case study. The degree of complexity is also variable, from more elementary solutions to more complex methodologies, especially in recent years.

On the other hand, although the research does not directly deal with these issues, it is important to have as context the studies that addresses the typological definition of elements for segmentation and classification based on point clouds, for the automatic classification of 3D data [13,14]. In that context, some works deal with the specific application of those strategies in architectural heritage [15,16]. Focused on columns, it is of interest the works [17,18], where the semantic characterization based on morphological similarities allows the definition of simplified geometric reconstructions of columns, and the methods used makes it possible to evaluate geometric deviations of each element in the collection.

The research focuses on analysing a specific architectural element: the column. It is a basic element of great conceptual simplicity while also offering a plethora of compositional solutions. Five basic typologies have been established, representing the most common column types that can be found in historic buildings. These typologies are defined based on the formal characteristics derived from their sections. Of course, this classification does not aim to encompass the entirety of possible typologies, as mentioned earlier, since the richness of formal solutions can be very varied. Therefore, the application of the proposed solutions to other case studies would require a prior typological study to avoid confusing accidental anomalies with those that may be intentional.

The proposed methodology builds upon previous work related to the formal analysis of masonry structural elements such as columns, vaults and arches [19-21] and also [22,23], among others.

2. Research aim

The aim of the research is to systematize an easy and accessible workflow, based on existing tools, to analyse column formal anomalies. The investigation is focused on ancient columns, but could be perfectly used in modern elements.

To ensure accessibility and ease of use for all users, the study is conducted with limited computing resources, primarily relying on the open-source software CloudCompare (V2.12.4) for point cloud processing. Supplementary calculations are performed using a worksheet (Open Office 4.1.11) and Matlab (MathWorks, R2022a Update 1).

3. Materials and methods

3.1. Study sample

The methodology is defined by directly working with the point clouds of the columns acquired from the terrestrial laser scanner, so potential errors arising from meshing processes are avoided. The analysis approach must be adapted to accommodate the variety of basic sections that can be found in ancient buildings. The study proposes a representative sample of pillars with the most common sections: round, square, octagonal, and clustered. A fifth subtype is considered, named irregular, for cases in which, despite having a basic geometric shape (in the case analysed, rounded), the physical reality presents significant discrepancies with respect to that shape. In addition, the survey exhibits relevant heterogeneities in terms of point cloud density.

A sample of 4 pillars (representing those that define a structural span of a bay) has been selected for each type (named by letters from a to d, ie. *Pa, Pb, Pc, Pd)* of the following Spanish buildings: churches of Bossòst, Castelló d'Empúries and Batea, and the Cathedrals of Mallorca and Tortosa. Due to the presence of capitals and/or bases with sculptural motifs, the analysis focuses on the shaft of the pillars.

The survey of Bossòst, Batea and Tortosa was carried out with the Leica ScanStation P20 scanner (Lluis i Ginovart, Coll-Pla, Costa-Jover 2014 campaigns), while in Mallorca and Castelló the Leica RTC360 scanner was used (Coll-Pla, Costa-Jover, Moreno Garcia, Samper-Sosa 2020 and 2022 respectively). The point cloud of each pillar was obtained in the context of the general survey of the buildings. The criteria for selecting the number of stations was the same in all buildings. A minimum of 4 stations are performed on each column to ensure that there are no occlusions. The point cloud is complemented with other nearby stations, in the process of surveying the rest of the building.

The accuracy of the P20 scanner is 6 mm at 50 m. In these scans, a combination of Black&White and reflective targets was used to perform the cloud-to-cloud alignment with the Cyclone program, and the resulting average cloud-to-cloud register error is 3 mm. In the case of the RTC360 scanner, the precision is 5.3 mm at 40 m, therefore, comparable to the previous case, and the alignment between clouds is done automatically with the Leica Cyclone Register 360 program, where the average register error between clouds in Castelló d'Empúries is established at 2 mm, while in Mallorca it is 4 mm.

Before analysing the pillars from the point clouds, the following processes are carried out:

- Manual segmentation of each column.
- Subsample and Resample establishing a minimum space between points of 0.005 m (according to the average resolution of the TLS used).
- Manual segmentation of each column shaft.
- Cleaning of noise points with the CloudCompare tool Noise Filter (the absolute maximum error is set to 0.02 m)
- Manual cleaning of outlier points and adjacent elements.

To obtain an initial approximation of the dimensional characteristics of the columns shaft, in relation to the point clouds, the main dimensional (height and area of the central section) and the number of points is recorded in the following steps: the number of original points for each complete pillar, the number after applying subsampling, and the number of points in the stem after noise reduction and manual cleaning (see Table 1). For the so-called irregular pillars, subsampling was not applied, as the original point cloud already exhibited very low point density.

Based on the resulting points and the surface area, it is possible to approximate the resolution of each column. The typology with a lower average resolution is the clustered, with 8913 point/m^2, while the typology with the highest resolution is the octagonal, with 19,509 point/m^2.

3.2. Analysis parameters

The identification and parameterization of formal anomalies in historical constructions poses a challenge, as there is often limited information about the initial shape, making it necessary to establish a hypothesis about a reference shape. These anomalies may result from errors during the setting-out or construction process, or

Table 1
Main characteristics related to dimensions and number of points for each column.

	Height (m)	Avg. Area (m^2)	Nº of original Points	Nº of subsample Points	Percentage OP-SP (%)	Nº of clean Points	Avg. resolution (point./m2)
Irregular							
Pa	3.405	0.80	239,970	–	–	193,282	15,877
Pb	3.302		278,951	–	–	217,782	
Pc	3.340		167,428	–	–	128,915	
Pd	3.233		210,209	–	–	158,302	
Round							
Pa	10.646	0.86	9,778,847	995,690	10.18	607,091	20,094
Pb	10.611		9,487,277	949,753	10.01	704,364	
Pc	10.574		10,384,558	997,701	9.61	721,068	
Pd	10.597		9,468,487	945,540	9.99	703,746	
Square							
Pa	7.33	1.33	1,181,659	861,382	72.90	503,701	12,884
Pb	7.355		1,085,732	829,523	76.40	488,198	
Pc	7.350		1,135,511	828,531	72.97	453,742	
Pd	7.399		1,197,243	798,272	66.68	431,582	
Octagonal							
Pa	20.488	2.35	21,565,393	4,249,940	19.71	2,791,040	19,510
Pb	20.62		24,009,436	4,441,892	18.50	2,618,387	
Pc	20.473		19,160,685	3,926,646	20.49	2,380,896	
Pd	20.602		22,274,951	4,466,484	20.05	2,520,805	
Clustered							
Pa	10.350	2.37	958,833	831,632	86.73	666,753	8913
Pb	10.354		1,080,607	937,697	86.78	743,034	
Pc	10.349		705,130	617,184	87.53	488,068	
Pd	10.155		702,713	593,000	84.39	466,465	

they may have occurred after construction due to settlement processes, interactions with nearby elements, or accidental incidents.

For the analysis of columns, certain assumptions can be made: that the base has not experienced horizontal displacements, that they were built to plumb, and that their vertical development was uniform (unless intentional changes in the section were made according to their typology or design).

The relevant alterations considered for the analysis are buckling and bulging. Buckling is understood as the displacement relative to the longitudinal axis of the entire section of the column. This displacement can occur in multiple forms, depending on factors such as the monolithic nature of the column or the restraint at the ends, together with the load conditions. Buckling occurs when the column bends outward relative to its central axis, resulting in a horizontal section that is larger than the initial one. In columns, we can also find the phenomenon of torsion, which refers to the rotation or twisting experienced by a structural column around its longitudinal axis. Torsion is not analysed, as its incidence is much lower compared to the other parameters under examination. Settlements have also been excluded from the analysis, as their detection requires a more comprehensive investigation, while the current focus is on specific examples. (Fig. 1) summarizes the workflow for the analysis developed.

3.2.1. Buckling

The buckling alteration in columns induces transverse displacements in the main direction of compression. It can manifest in various ways, with the type of structural union at the ends playing a decisive role, along with other dimensional parameters. In cases where the base is fixed and the upper end is free, the deformation can result in a loss of verticality at the top. In the study, these formal anomalies will be characterized based on distances and angles.

For the analysis, sections of points at different heights are used. The study directly operates with the coordinates of the points comprising these sections, after cleaning the point clouds to eliminate outliers that could distort the results.

The sections are defined by manually segmenting the point cloud of each pillar, dividing it into four equal parts. It is considered that 4 parts are the minimum to identify anomalies along the height of columns, as it establishes a “checkpoint” on each half (top and bottom) of the column. Depending on the magnitude and location of possible anomalies identified, or the desirable accuracy of the study, it would be necessary to increase the number of sections (in the overall column or focused on a certain area) to be able to analyse the anomalies in greater detail, but the methodology would be the same.

Thus, five sections are obtained, including the base, top, and three intermediate ones. A step of 0.02 m is applied during the selection of points for each section to ensure an adequate number of points in each segment. Obviously, the criteria used to determine the number of sections are designed to facilitate result comparison among different pillars. In a specific case study, the number of necessary sections should be adjusted based on the state of the pillar (more or less altered) and its height.

To ensure consistency in analysing various shapes of pillars, it was decided to work based on the definition of the centroid of points within each horizontal section. The position of this centroid can be determined using different methods, and the reliability of the analysis will depend on the quality provided by each method.

Three methods to obtain the centroid are tested, seeking to optimize the relationship between the complexity of the process and the precision of the result. The proposed approaches, from least to most complex, are:

a) calculation of the arithmetic means of the coordinates (x, y) of the points in each section (spreadsheet)
b) calculation of the box containing each section (CloudCompare)
c) calculation of the conic that best approximates the points of each section (Matlab)

Once the centroid coordinates have been obtained by each method, and one is selected to carry out the analysis of buckling for each type of pillar. These are studied taking the centroid of the column base section as the reference point (0,0), and the distance between the reference point and the coordinates (x, y) of the centroid of each section is established. The centroids also allow you to establish the angle of the collapse, both in section and in plan.

Among the proposed methods, the first approach (a) is very elementary and does not involve any complexity. The second method

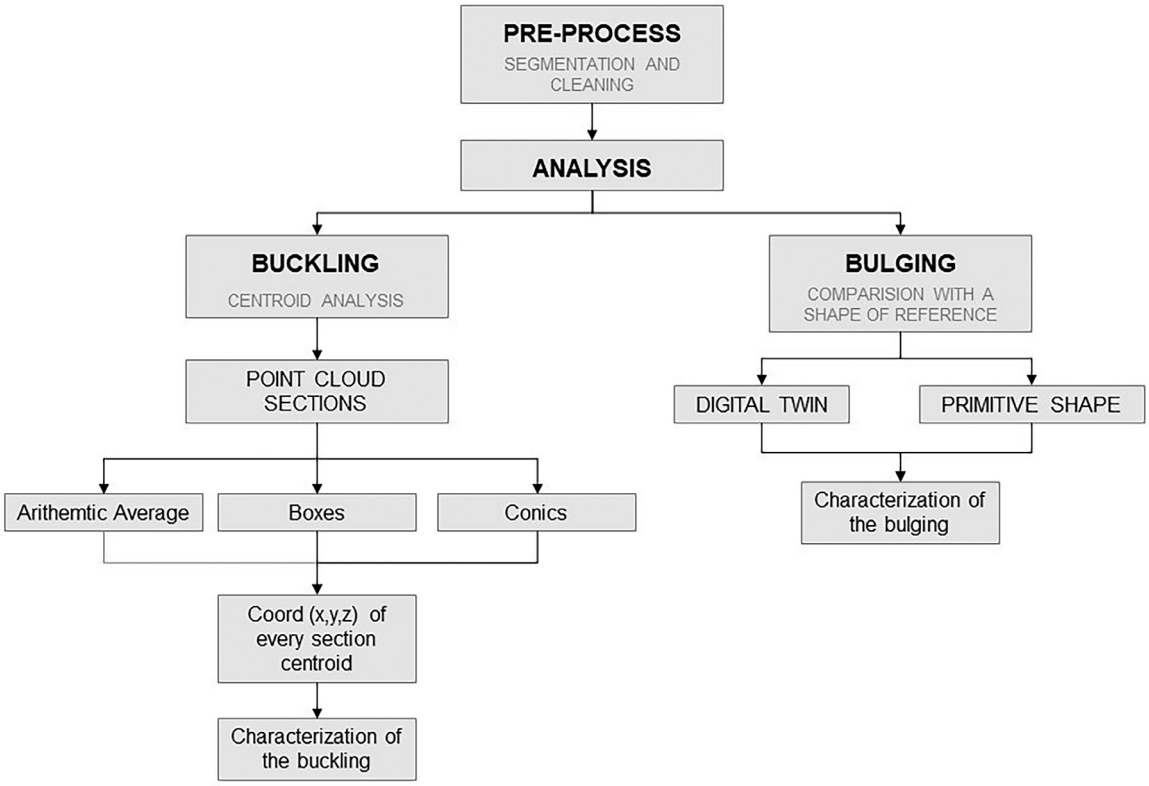

Fig. 1. Workflow for the analysis of buckling and bulging in columns.

(b) relies on the coordinates provided by the CloudCompare program for the bounding box containing the point cloud of each section. Both of these approximations offer a simple and rapid way to determine the centroid. Additionally, the calculation of the centroid using a script developed for Matlab, which involves adjusting conics to the points of each section, is described in detail.

A conic is the locus of the points in the (x, y) plane that satisfy a complete quadratic equation, whose general expression is the one collected in Eq (1).

$$\boldsymbol{Ax}^2 + \boldsymbol{By}^2 + \boldsymbol{Cxy} + \boldsymbol{Dx} + \boldsymbol{Ey} + \boldsymbol{F} = \boldsymbol{0} \tag{1}$$

For each of the points of each section at different heights, an equation of this type is proposed, and later the system is solved by least squares, so that information on the goodness of the adjustment made can be available.

Next, the results obtained were analysed using different statistical tests based on the covariance matrix of unknowns and observables, and the residues of the latter, eliminating those points considered as gross errors or noise, and recalculating the solution for each section.

Once we have the definitive values, we proceed to classify the conic, and obtain its axes, centre, and rotation if applicable. To do this, we base ourselves on the matrix expression proposed once the coefficients of the curve are known, Eq (2).

$$(1\ \boldsymbol{x}\ \boldsymbol{y}) \begin{pmatrix} \boldsymbol{a}_{00} & \boldsymbol{a}_{01} & \boldsymbol{a}_{02} \\ \boldsymbol{a}_{10} & \boldsymbol{a}_{11} & \boldsymbol{a}_{12} \\ \boldsymbol{a}_{20} & \boldsymbol{a}_{21} & \boldsymbol{a}_{22} \end{pmatrix} \begin{pmatrix} 1 \\ \boldsymbol{x} \\ \boldsymbol{y} \end{pmatrix} = 0 \tag{2}$$

A conic is thus defined by a symmetric matrix. Starting from the invariants and the attached matrices $\boldsymbol{A_{ii}}$ we proceed to obtain all the values, as well as the centre/pole and the diameters, in those that are possible, Eq (3).

$$\boldsymbol{a}_{00} = \boldsymbol{F},\ \boldsymbol{a}_{11} = \boldsymbol{A},\ \boldsymbol{a}_{22} = \boldsymbol{B},\ \boldsymbol{a}_{12} = \boldsymbol{a}_{21} = \frac{\boldsymbol{C}}{2},$$

Table 2
Synthesis of the results and comparison of the centroid coordinates obtained by the three methods: conics (CON), boxes (BOX), an arithmetic mean (MED).

		Difference between CON-BOX (m)	Difference between CON-MED (m)
Irregular	mean	0.003	0.120
	min.	0.000	0.025
	max.	0.052	0.255
Round	mean	0.001	0.008
	min.	0.000	0.001
	max.	0.007	0.041
Square	mean	0.012	0.070
	min.	0.004	0.028
	max.	0.051	0.131
Octagonal	mean	0.007	0.044
	min.	0.001	0.021
	max.	0.028	0.115
Clustered	mean	0.004	0.100
	min.	0.000	0.010
	max.	0.015	0.365
	Global mean	**0.005**	**0.068**
	Global min.	**0.000**	**0.001**
	Global max.	**0.052**	**0.365**

$$\boldsymbol{a}_{01} = \boldsymbol{a}_{10} = \frac{\boldsymbol{D}}{2},\ \boldsymbol{a}_{02} = \boldsymbol{a}_{20} = \frac{\boldsymbol{E}}{2} \tag{3}$$

The conics can be classified as follows:

- Ellipse:
  - Real
  - Imaginary
- Hyperbola
- Parabola
- Pairs of lines:
  - No real parallels
  - No imaginary parallels
  - Real parallel or matching lines

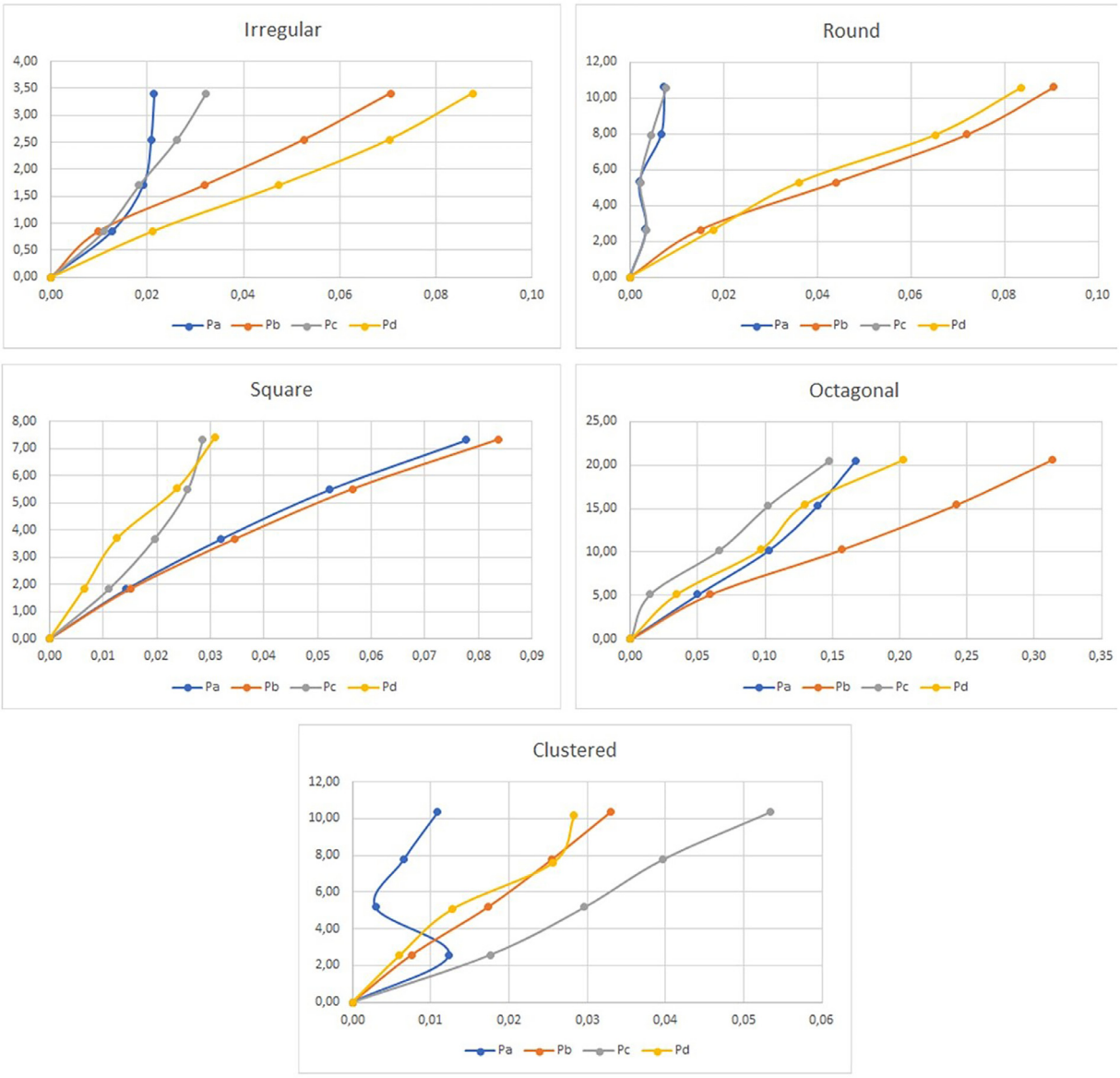

Fig. 2. Graphs of the results of the buckling distances (m) obtained in each pillar.

- Imaginary parallels
- Matching lines

Starting from the general equation of a conic, its reduced equation can be reached by consecutively applying a rotation and a translation in an appropriate way.

The reduced equation of a conic is a simplified equation of the curve that locates the centre (if it exists) of the conic at the origin of coordinates, while the axes have specific relations with the conic. In the case at hand, it would be ellipses with general equation, Eq (4).

$$a''_{00} + a''_{11}x^2 + a''_{22}y^2 = 0 \quad (4)$$

For all columns, sections with sufficient resolution and point density were available to consider them complete. Therefore, for all cases an ellipse can be calculated as a conic since it is a closed set. Even so, we worked adjusting the general equation of the conics (Eq. (2)), with equation systems with a high degree of redundancy. After classification we verify that the conic is an ellipse. From the coefficients, Eq. (2) and Eq. (3). the centre can be obtained. Actually, this is the parameter that we need to compare to the other methodologies applied in the study.

3.2.2. Bulging

When buckling occurs, it manifests across the entire section, resulting in anomalies on one side of the column corresponding to those on the opposite side. We will speak of 'bulging' when this alteration in the vertical development occurs only on one side.

The sections carried out in the study of buckling provide an initial approximation to the problem but offer only partial information. As a result, the developed analysis focuses on exploring the possibilities of conducting a 3D study.

Thus, the analysis of bulges is carried out by comparing the point cloud with a reference shape that makes it possible to identify and quantify the alterations. Two analysis methods are proposed in function of the procedure to define the reference form, which in both cases will be a 3d mesh:

- Analysis from a digital twin
- Analysis from a primitive form of reference

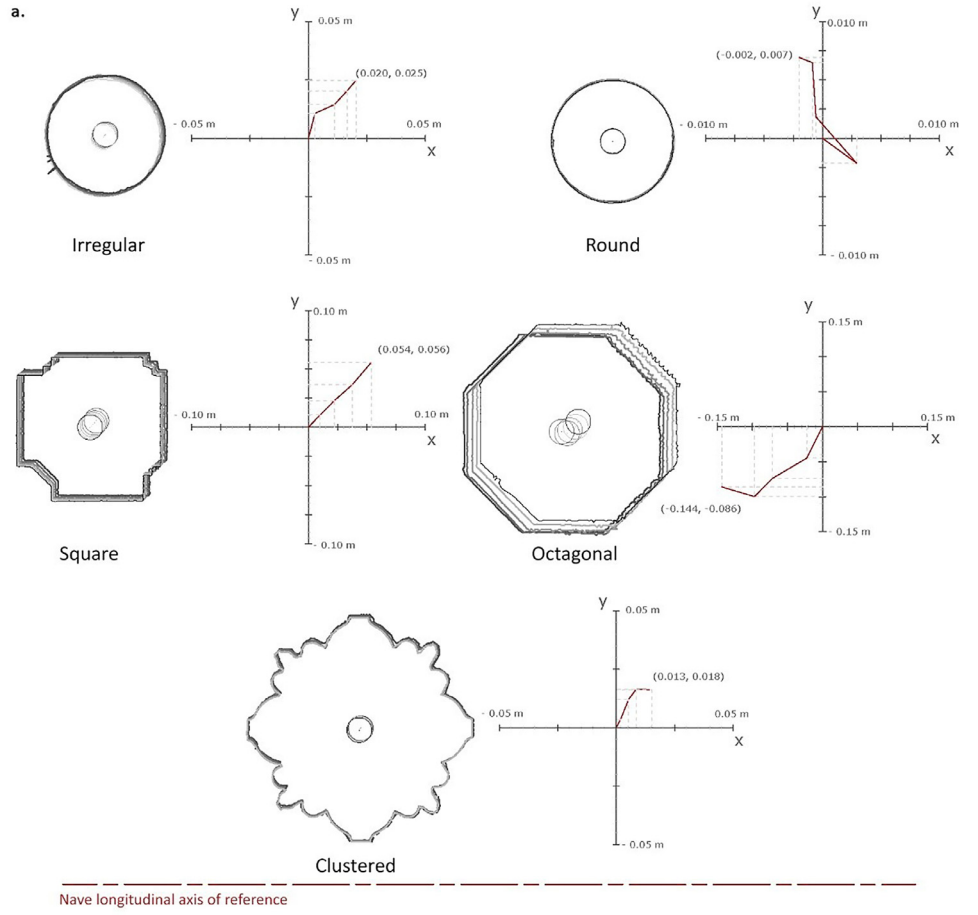

Fig. 3. Buckling representation in floor plant: a) plan representation of the centroids from the overlap of each section; b) example of representation contextualized in the building, of the direction of the buckling.

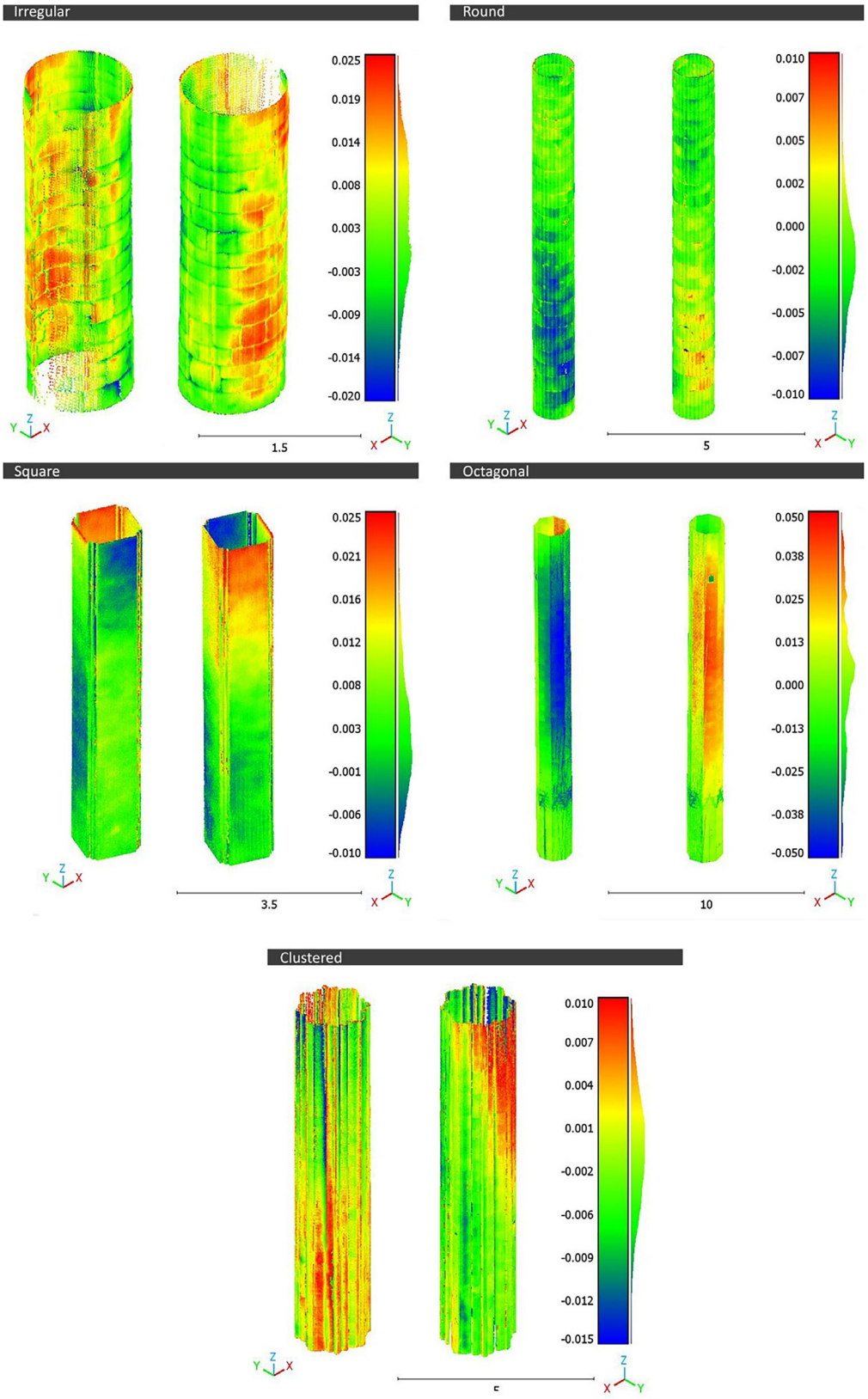

Fig. 4. Results for each type of pillar, from the comparison between the point cloud and the digital twin.

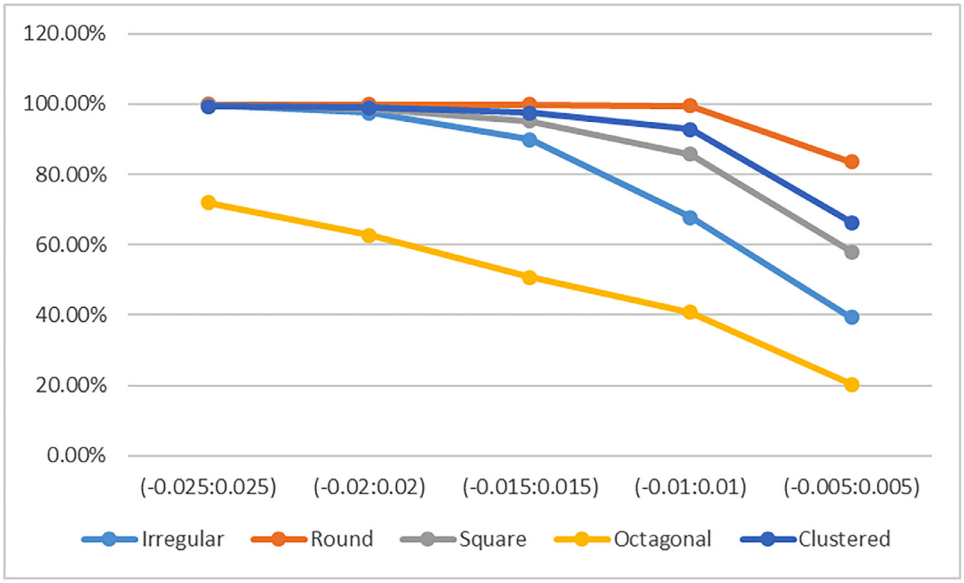

Fig. 5. Analysis of the distance ranges (in meters) between the digital twin and the point cloud, based on the histograms of each pillar.

When creating a digital twin, the existence of a buckling must be taken into account, since it can mask the results of the analysis by altering the vector from the centre of mass. In order to minimize the distance between the point cloud and the digital twin, this is generated from the section at the base of the column and is developed in height from the vector resulting from joining the centroids of the extreme sections.

Additionally, the analysis based on primitives is a consolidated method (see references in the Introduction section). In this study, we have chosen to use robust methods, as is the well known Random sample consensus (RANSAC) method [24].

Once the reference shape is obtained by these both methods, the distances between said shape and the point cloud are calculated. In this way, it is possible to analyse the results obtained by these methods. The analysis based on reference primitives is not applicable in the case of clustered columns, due to their formal complexity.

4. Results

4.1. Buckling analysis

As previously introduced, the buckling analysis involves calculating the centroids of different sections in each column. First, the centroid coordinates obtained for each column using the three proposed methods are studied and compared between conics and boxes (CON-BOX) and conics and arithmetic mean (CON-MED). Table 2, summarizes the results obtained, indicating the maximum and minimum differential distances (in absolute value), and the mean value of the difference in each set of columns (irregular, round, square, octagonal and clustered).

If we analyse the differences between the calculation of the centroid using different methods, the total mean difference when comparing conics with boxes (CON-BOX) is 0.005 m, with a range of values of [0.000, 0.052 m]. On the other hand, when comparing conics with the arithmetic mean (CON-MED) the mean difference is 0.068 m, and the range of values is [0.001, 0.365 m].

The difference in the first case (CON-BOX) is considered negligible, as it corresponds to the measurement noise itself, (avg.= 0.005 m). However, the calculation using the mean (CON-MED) results in larger discrepancies (avg.= 0.068 m). These results can be attributed to the lack of homogeneity in the point cloud. The highest differences are observed in the case of irregular columns, with a mean difference of 0.120 m, and slightly lower, 0.100 m, for clustered columns. These typologies exhibit greater heterogeneity in the distribution of points due to the data collection and the geometry of the column (variation of the radial distance). This evidences that the calculation of the centroid through the arithmetic mean is highly sensitive to the distribution of points, making it less reliable in unfavourable cases.

Next, the buckling of each pillar is analysed based on the results obtained from the conical method. The analysis involves defining the horizontal displacement vector of each centroid and its angle of inclination with respect to the vertical plane. These parameters enable the identification of whether the buckling occurs homogeneously (linear throughout all the height), or heterogeneously (it can be progressive or irregular).

The coordinates of the centroid at the base are considered the reference point (0,0). From there, the horizontal displacement vector of each centroid with respect to the reference point (0,0) and the angle formed by the displacement in relation to the vertical axis are determined.

Fig. 2 displays the results obtained in each column. For each section, the height, buckling value, and angle with respect to the vertical are specified. Naturally, the maximum buckling value is found in the upper sections, specifically in the Pb pillar of the octagonal typology, which is the tallest at >20 m. On the other hand, the steepest angle is observed in the Pb column of the irregular typology. Despite its height being just over 3 m, this inclination does not lead to a large leaning.

In the cases of the irregular, round, and square typologies, noteworthy patterns emerge in the distance measurements, grouping the columns according to where they are located. To interpret the results from a qualitative point of view, it is necessary to understand the context of the columns, located in the central nave of the buildings. According to the central axis of the nave, the columns Pa and Pc are located on one side, and the pillars Pb and Pd are on the opposite side. According to the results of the analysis, the pillars located on the same side present similar inclinations, both partial and total.

The provided information quantifies the buckling regardless of its direction. A plan representation (Fig. 3a) is used to indicate the displacement with respect to the base point (0, 0) by operating graphically from the centroids' coordinates in (x, y) of each section.

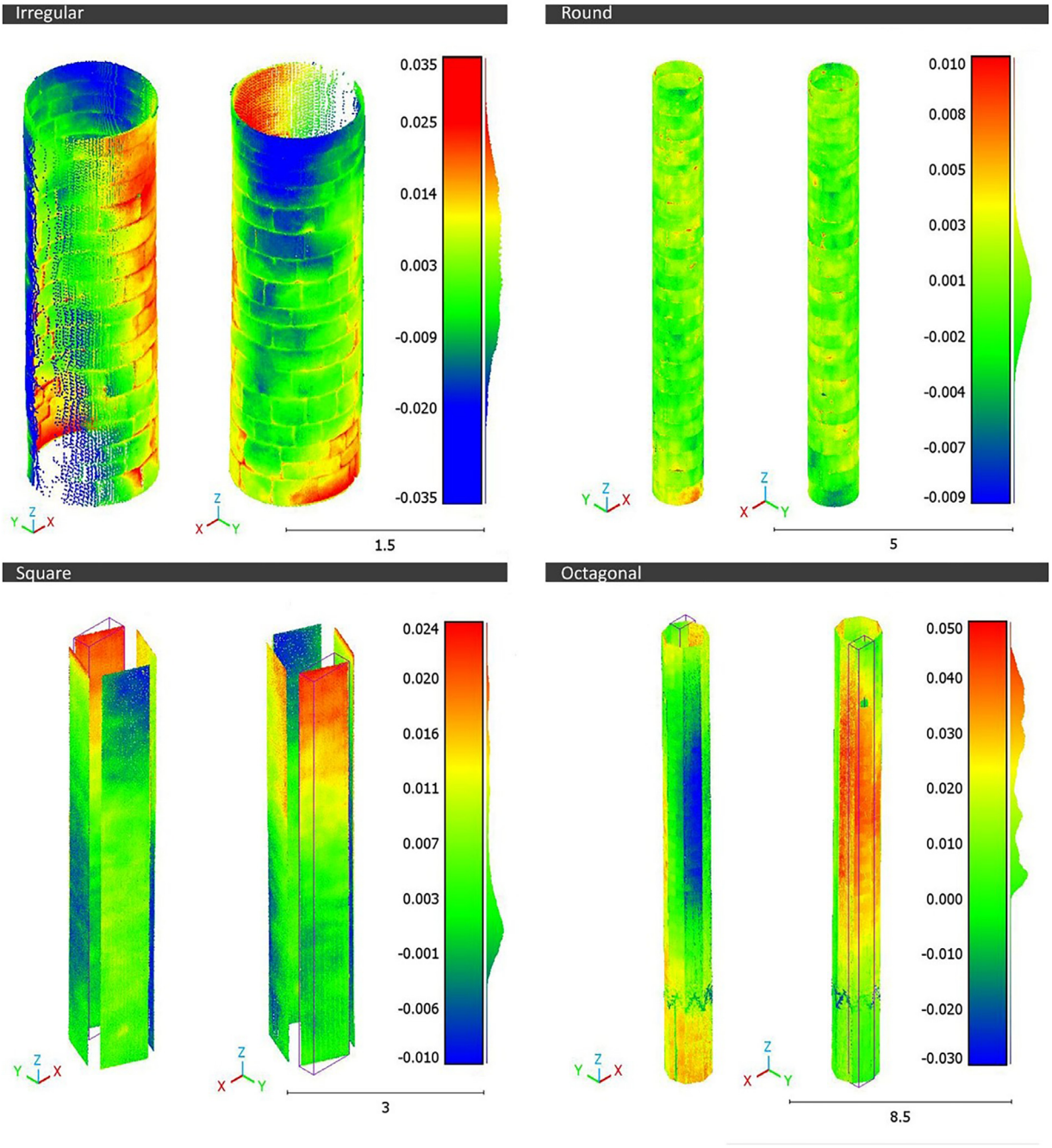

6. Results of the comparison between the point cloud and the primitives. In Square and Octagonal typologies, only the histogram of the indicated plane is displayed.

Fig. 3b illustrates an example of representation within the context of a building, indicating the direction of the inclination relative to the longitudinal axis of the structure. The longitudinal axis of the nave is determined from the centroids of the four pillars, and the angle of the point buckling vector with respect to this axis is indicated. This angle represents the horizontal component of the vector resulting from joining the coordinates (x, y) of the end sections of each pillar.

4.2. Bulging analysis

The bulge analysis is tested using two different methods to obtain the reference shape: digital twin modelling from the end sections and primitive shapes obtained by the RANSAC method in CloudCompare.

Below are the distance maps obtained from the comparison of the point cloud with its digital twin for each type of pillar. The visualization of the distance ranges in each typology has been optimized for the detection of formal anomalies (Fig. 4).

The generated images allow the identification of formal anomalies in the column shaft, but they require interpretation. It is important to verify if there is correspondence between opposite sides, as it indicates the existence of buckling:

- Irregular: this typology exhibits great discrepancies with respect to the digital twin, and no correspondence between sides is observed.
- Round: this typology shows the highest level of agreement between the point cloud and the digital twin. The identified anomalies have correspondence between opposite sides.

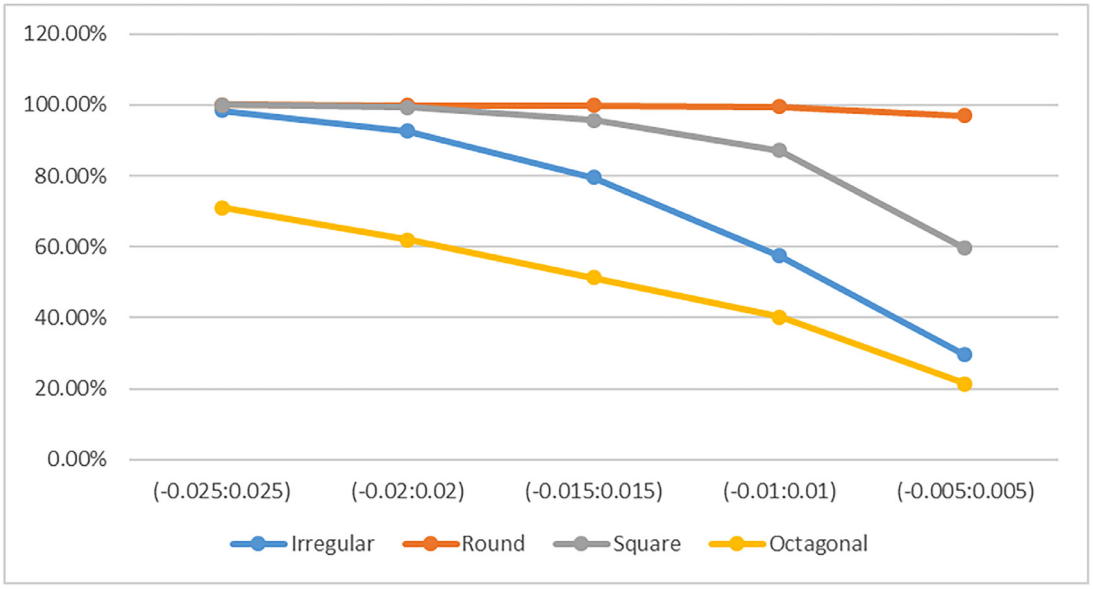

Fig. 7. Analysis of the distance ranges (in meters) between the primitive shape and the cloud of points, based on the histograms of each pillar.

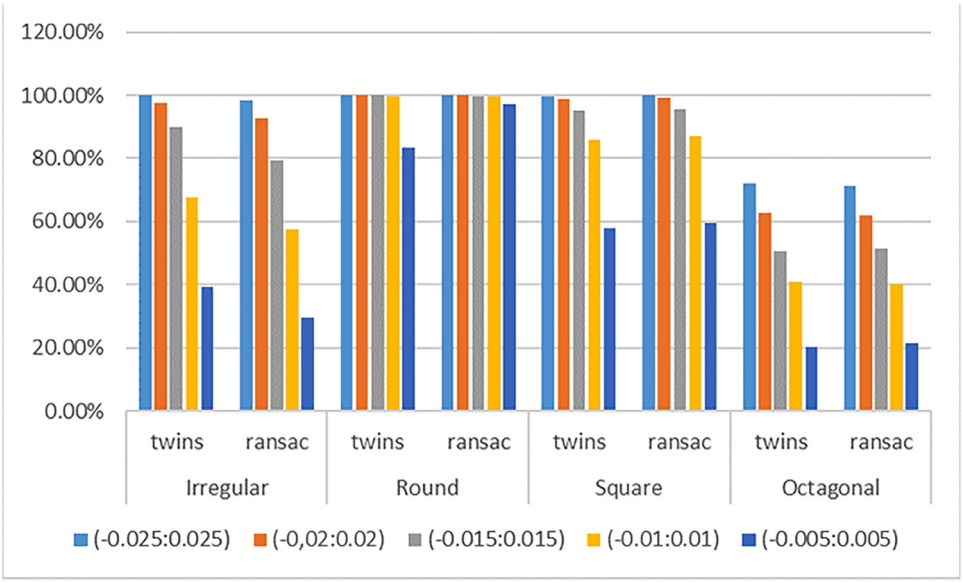

8. Comparison of the results obtained by the two proposed methods (digital twins – RANSAC primitives). In the case of the results obtained by Ransac primitives, in the square and octagonal pillars the mean of the percentages in each plane analysed is shown for each range.

- Square: the main differential distances are found in the upper part of the column, with correspondence between sides. However, small discrepancies (around 0.01 m) are also identified approximately in the middle of the shaft.
- Octagonal: this typology experiences the greatest discrepancies due to the buckling it presents, a consequence of the column's significant height. There is correspondence between sides.
- Clustered: Various areas with discrepancies without correspondence on the opposite side are identified. It is important to note that the values are of small magnitude (−0.015 m to 0.010 m).

It should also be noted that the distances in all cases are small on an architectural scale, on the order of centimetres (Fig. 5). At least 99.41% of the values do not exceed the range [−0.025, 0.025 m] in any typology, except for the octagonal typology where the percentage of points falling within the range is 71.99%. The latter exhibits greater discrepancies due to the existence of the aforementioned buckling in the central third, and it is also the column that notably exceeds the height of the rest of the study cases.

Next, we present the results obtained through primitive forms. The primitives were obtained using the Ransac Shape Detection plug- in the CloudCompare program. For the irregular and round typologies, the cylinder primitive was used, while for the square and octagonal types, we sought the plane that best approximates each face. The clustered pillar has not been analysed due to its formal complexity.

Fig. 6 displays the distance maps on the point cloud obtained, where the level of coincidence can be observed in relation to those obtained with the digital twin:

- Irregular: the range of distances is significantly greater than with the digital twin, and the distribution of the greater distances is not coincidental.
- Round: the range of distances is still very small [−0.010, 0.010] compared to the analysis with respect to the digital twin, and

most of the points are within a range of millimetres. Even so, the distance distribution is not coincident with respect to the digital twin.
- Square: both the range of distances and their distribution is very similar in both cases.
- Octagonal: due to the distance ranges obtained in each plane, it is not possible to match the display parameters. Despite this, the distribution of values is very similar between both methods.

In the case of the octagonal typology, notable differences are identified in the distribution of points based on the range of distances in each comparison plane. This distribution varies among different planes. Some planes have a high percentage of points in the higher distance ranges [−0.025, 0.025] and [−0.020, 0.020], but then the percentage is smaller for small ranges. These differences can be related to the already established existence of a relevant inclinations.

In the same way as in the previous method, the distances are still small, in architectural terms, of the order of centimetres (Fig. 7). The relative distribution of the points according to rank, although similar, does not coincide with the digital twin method (this fact is analysed in more detail below), and the octagonal typology continues to be the one that presents the greatest differences between the cloud of point and the reference form.

When comparing the distance ranges obtained by the two methods (Fig. 8), we observe that, in general terms, there is no significant difference between them:

- Irregular: the correspondence with the point cloud is noticeably lower with the method using graphic primitives.
- Round: the values are practically the same, with the percentage of points in the range [−0.005, 0.005] being slightly smaller in the case of the digital twin.
- Square: the differences in the percentage distribution of points for each range of distances in this case are negligible.
- Octagonal: as in the previous case, the differences are also very small.

5. Discussion and conclusions

The research has systematically characterized the main formal anomalies in pillars from point clouds, proposing a simple and accessible methodology using readily available software. In general terms, the proposed approach is applicable to all types of pillars and columns without the need to adapt the processes to specific typologies commonly found in historic buildings, especially in the case of buckling. However, it is important to acknowledge that the selected cases for analysis have been chosen based on typological considerations, specifically focusing on instances where the section remains unaltered intentionally all over its height. Therefore, a typological characterization is imperative in all instances to determine the suitability of the study methods.

In relation to buckling, testing different procedures for calculating the centroid of each pillar at different heights revealed that the arithmetic mean method is more sensitive to the density of the point cloud than the other two methods. As such, it is not considered adequate. Between calculating the centroid from the conic that best approximates the section (CON) and from the box that contains it (BOX), the differences in metrics are very small (considering architectural elements). Although it is difficult to specify the best process in this case, the conical method offers more methodological guarantees, despite requiring more time investment.

In terms of time consumption for obtaining centroids using different methods, once the points from each section are isolated, the box method is immediate, as CloudCompare itself allows direct visualization of the information. The arithmetic mean and conic methods require importing coordinates and then performing the relevant calculations, with the mean method being very fast, while with conics, it's necessary to prepare the coordinate file beforehand. This results in higher time consumption compared to the box method, especially in the case of conics. Once the centroid coordinates are obtained, they need to be manually input into the spreadsheet to calculate the deflections.

Regarding the characterization of buckling, the calculation of the centroid has proven to be a sound strategy, allowing for a simple and valid operation across all types of columns. The identified buckling values are small from an architectural perspective, except for the octagonal typology. The study enables the identification and tracking of anomalies and their progression, along with determining the direction, which is relevant information that can be related to anomalies in other construction elements in a comprehensive study, with significant implications from a mechanical perspective.

Though it was not the main objective of the investigation, the documentation provided also makes possible the identification and quantification of torsion in polygonal (square and octagonal) and clustered pillars. This type of anomaly has not been observed in the cases analysed, but if it had existed, it would have been evidenced in the superposition of the sections, through the differences in position between the edges of each section.

Regarding bulges, the two proposed methods (digital twin and primitive shape) enable the identification and visualization of affected areas in three dimensions. Buckling deformations are also distinguishable from bulges based on whether the anomaly affects only one side of the column or both.

There is no significant difference between the two methods in terms of the distribution of points according to ranges of distances. For clustered columns, obtaining a reference shape is limited to the proposed method of defining a digital twin. From the time consumption standpoint, analysing columns that can be assessed as cylinders is considerably fast in both cases, with perhaps the digital twin modelling being slightly slower. However, in the case of columns with flat faces, the use of primitives results in a greater time consumption, as each face must be analysed independently, while providing the benefit of independent analysis for each plane. In this case, digital twin modeling turns out to be faster, as it can generate all the faces at the same time.

Acknowledgements

The survey of Mallorca Cathedral was promoted and financially supported by the Cabildo de la Catedral de Palma de Mallorca (T20278S).

The survey of the Castelló d'Empúries church was supported by the Bisbat de Girona, and counted with the financial support of the Ajuntament de Castelló d'Empúries (T22284S).

This work is framed in the research project "Smart Built Heritage. Del registro a la simulación digital para inmuebles medievales y modernos" (TED 2021-129148B).

The authors Agustí Costa-Jover and Sergio Coll-Pla are Serra Hunter fellows.

Supplementary materials

Supplementary material associated with this article can be found, in the online version, at doi:10.1016/j.culher.2024.04.017.

References

[1] R. Kadobayashi, N. Kochi, H. Otani, R. Furukawa, Comparison and evaluation of laser scanning and photogrammetry and their combined use for digital recording of cultural heritage, Int. Arch. Photogramm. (2004).
[2] P. Grussenmeyer, T. Landes, T. Voegtle, K. Ringle, Comparison methods of terrestrial laser scanning, photogrammetry and tacheometry data for recording of cultural heritage buildings, Int. Arch. Photogramm. Remote Sens. Spat. Inf. Sci. 37 (B5) (2008) 213–218.

[3] S. Martínez, J. Ortiz, M.L. Gil, M.T. Rego, Recording complex structures using close range photogrammetry: the cathedral of Santiago De Compostela, Photogramm. Rec. 28 (144) (Dec. 2013) 375–395, doi:10.1111/phor.12040.
[4] F. Fassi, C. Achille, L. Fregonese, Surveying and modelling the main spire of Milan Cathedral using multiple data sources, Photogramm. Rec. 26 (136) (Dec. 2011) 462–487, doi:10.1111/j.1477-9730.2011.00658.x.
[5] F. Pirotti, Open software and standards in the realm of laser scanning technology, Open Geospatial Data, Softw. Stand. 4 (1) (2019), doi:10.1186/s40965-019-0073-z.
[6] E. Quagliarini, P. Clini, M. Ripanti, Fast, low cost and safe methodology for the assessment of the state of conservation of historical buildings from 3D laser scanning: the case study of Santa Maria in Portonovo (Italy), J. Cult. Herit. (2016), doi:10.1016/j.culher.2016.10.006.
[7] E. Bonali, A. Pesci, G. Casula, E. Boschi, Deformation of ancient buildings inferred by terrestrial laser scanning methodology: the Cantalovo church case study (Northern Italy)*,", Archaeometry 56 (4) (Aug. 2014) 703–716, doi:10.1111/arcm.12028.
[8] G. Vacca, F. Mistretta, F. Stochino, A. Dessi, Terrestrial laser scanner for monitoring the deformations and the damages of buildings, Int. Arch. Photogramm. Remote Sens. Spat. Inf. Sci. - ISPRS Arch. 41 (2016) 453–460 no. June, doi:10.5194/isprsarchives-XLI-B5-453-2016.
[9] M. Korumaz, et al., An integrated terrestrial laser scanner (TLS), deviation analysis (DA) and finite element (FE) approach for health assessment of historical structures. A minaret case study, Eng. Struct. 153 (2017) 224–238 no. July 2016, doi:10.1016/j.engstruct.2017.10.026.
[10] J. Sun, B. Peng, C.C. Wang, K. Chen, B. Zhong, J. Wu, Building displacement measurement and analysis based on UAV images, Autom. Constr. 140 (2022) 104367 no. December 2021, doi:10.1016/j.autcon.2022.104367.
[11] E.M. Mouaddib, A. Pamart, M. Pierrot-Deseilligny, D. Girardeau-Montaut, 2D/3D data fusion for the comparative analysis of the vaults of Notre-Dame de Paris before and after the fire, J. Cult. Herit. 65 (2023) 221–231, doi:10.1016/j.culher.2023.06.012.
[12] J. Moyano, I. Gil-Arizón, J.E. Nieto-Julián, D. Marín-García, Analysis and management of structural deformations through parametric models and HBIM workflow in architectural heritage, J. Build. Eng. 45 (2022) no. September 2021, doi:10.1016/j.jobe.2021.103274.
[13] F. Poux, J.J. Ponciano, Self-learning ontology for instance segmentation of 3d indoor point cloud, Int. Arch. Photogramm. Remote Sens. Spat. Inf. Sci. - ISPRS Arch. 43 (B2) (2020) 309–316, doi:10.5194/isprs-archives-XLIII-B2-2020-309-2020.
[14] J.-J. Ponciano, M. Roetner, A. Reiterer, and F. Boochs, "Comparison of a deep learning and a knowledge-based method," 2021, [Online]. Available: https://doi.org/10.3390/ijgi10040256.
[15] E. Grilli, F. Remondino, Classification of 3D digital heritage, Remote Sens 11 (7) (2019) 1–23, doi:10.3390/RS11070847.
[16] R. Pierdicca, et al., Point cloud semantic segmentation using a deep learning framework for cultural heritage, Remote Sens 12 (6) (2020) 1–23, doi:10.3390/rs12061005.
[17] D.Lo Buglio, V. Lardinois, L. De Luca, Revealing shape semantics from morphological similarities of a collection of architectural elements: the case study of the columns of Saint-Michel de Cuxa, in: *Proc. Digit. 2013 - Fed. 19th Int'l VSMM, 10th Eurographics GCH, 2nd UNESCO Mem. World Conf. Plus Spec. Sess. fromCAA, Arqueol. 2.0 al.*, vol. 1, 2013, pp. 465–472, doi:10.1109/DigitalHeritage.2013.6743785.
[18] A. Pamart, D. Lo Buglio, L. De Luca, A. Pamart, D. Lo Buglio, and L. De Luca, "Morphological analysis of shape semantics from curvature-based signatures To cite this version : HAL Id : hal-03629167 Morphological Analysis of Shape Semantics from Curvature-based Signatures," 2022.
[19] J. Lluis i Ginovart, S. Coll-Pla, A. Costa-Jover, M.L. Piquer, Evaluation of large deformations on Romanesque masonry pillars: the case of Santa María de Arties (XII-XIII) at Valle de Arán, Spain, Rev. la Constr. 16 (3) (2017) 468–478, doi:10.7764/RDLC.16.3.468.
[20] J. Lluis i Ginovart, A. Costa-Jover, C. Lluis-Teruel, D.García Moreno, S. Coll-Pla, Geometric anomalies in the construction of tile vaults in the Hall Temples the Hall Temples the 18th century: sant Miquel de Batea, Inf. la Constr. 74 (568) (2022), doi:10.3989/ic.91267.
[21] S. Coll-Pla, J. Lluis i Ginovart, A. Costa-Jover, C. Lluis Teruel, Acercamiento formal y estudio estructural de la arquitectura románica del Valle de Arán, Revistarquis 11 (1) (2021) 1–15, doi:10.15517/ra.v11i1.45646.
[22] A. Costa-Jover, J.M. Macias Solé, J.M. Puche Fontanilles, Structural deformations of the Visigothic church of Sant Miquel de Terrassa, Inf. la Constr. 71 (555) (2019), doi:10.3989/ic.66776.
[23] F. Buill, M.A. Núñez-Andrés, A. Costa-Jover, D. Moreno, J.M. Puche, J.M. Macias, Terrestrial laser scanner for the formal assessment of a roman-medieval structure—The cloister of the cathedral of Tarragona (Spain), Geosci 10 (11) (2020) 1–16, doi:10.3390/geosciences10110427.
[24] M.A. Fischler, R.C. Bolles, Random sample consensus: a paradigm for model fitting with applications to image analysis and automated cartography, Commun. ACM 24 (6) (1981) 381–395, doi:10.1145/358669.358692.